Study on the mechanism affecting the quality of micro-hole in ultrasonic-assisted drilling of high-speed circuit boards

Zhisen Gao
Hongyan Shi (shy-no.1@163.com)
Shenzhen University
Sha Tao
Xianwen Liu
Tao Zhu
Zhuangpei Chen

Research Article

Keywords: High-speed circuit board, Ultrasonic-assisted drilling, Micro-hole quality, Orthogonal Test

Posted Date: April 12th, 2022

DOI: https://doi.org/10.21203/rs.3.rs-1524941/v1

Abstract

High-speed circuit boards are created to meet the high-speed signal transmission requirements of 5G communication technology, but the non-polar resins, flat glass fibers, and multiple and hard fillers used for this purpose have launched new challenges to their micro-hole processing. Micro-hole quality has always been a decisive factor in board performance, therefore, this paper proposes a new processing method for improving micro-hole drilling quality of high-speed circuit boards, establishes an ultrasonic-assisted drilling tool motion model. Then, this paper analyzes the changes in drilling method, material deformation, chip breakage and chip removal during ultrasonic-assisted drilling of printed circuit boards, to study the influence mechanism on micro-hole quality during ultrasound-assisted drilling. In addition, an experimental platform for ultrasonic-assisted drilling is designed and built, and single-factor experiments for verification of ultrasonic effects, optimization of drilling parameters, and orthogonal experiments for ultrasonic-assisted drilling of high-speed circuit boards are conducted on this platform. The experimental results show that the loading of ultrasonic vibration has a very obvious improvement on the situation of several machining defects such as hole wall roughness, entrance burr and nail head in micro-hole drilling of high-speed circuit boards. In addition, the influence order and better level combination of each processing parameter are obtained, which provides a theoretical research basis and processing instructions for the improvement of micro-hole quality of high-speed circuit boards.

1. Introduction

In order to meet the high-speed signal transmission requirements of 5G communication technology, a high-speed circuit board with lower dielectric constant (Dk) and dielectric loss (Df) values than ordinary printed circuit boards (PCBs) has come into being, but the non-polar resins, flat glass fibers, and multiple and hard fillers used for this purpose have launched new challenges to their micro-hole processing. Therefore, the study of micro-hole drilling for high-speed circuit boards to ensure that their processing quality can meet the requirements of the times is an important issue raised by the development of 5G communication technology.

PCBs generally rely on metallized micro-hole to electrically connect different circuit layers, so the quality of micro-hole has always been the focus of scholars' attention. (20) summarized the technology development direction of high-speed circuit boards and the current status of raw material selection and application, which provides the basis for the processing mechanism research of high-speed circuit boards. Ko et al. (4) centered his research on micro-hole burrs and proved through experiments that the step drill is effective in improving the generation of micro-hole burrs. Bhandari et al. (2) design an experiment (DOE) technique based on the Taguchi method was used to find the most significant drilling parameter affecting burr height. The results show that the drill diameter makes a statistically significant contribution to burr-height variation. Song et al. (13) found that tool wear also reduces the hole accuracy of PCB drilling, which eventually leads to an increase in burr height and nail head Hidehito et al (15) experimentally verified the correlation between the radial runout of the drill and the micro-hole quality. Sahoo et al. (10) used finite element analysis (FEA) based deformation and stress simulation to obtain

the effect of feed rate on various parameters of micro-hole quality during PCB drilling. Other scholars have studied from the direction of drills, such as Wang et al. (14) who developed their own Ti-based cermet micro-drills for PCB hole processing. However, the drill is a processing consumable, and the way to enhance its cost to improve the hole quality is not as good as the improved processing method in terms of economic benefits. (12) pointed out in their study that with the development of communication technology, high-frequency and high-speed circuit boards are taking up an increasing share of the market. However, most of the above studies are based on traditional printed circuit boards, and the research on high-speed circuit boards is very fragmented and not deep enough.

Zhang et al. explained the essence of ultrasonic-assisted machining technology(17), which is a technique for machining with force loaded on the tool or workpiece in the form of high-frequency pulses, while Zhang et al.(19) also confirmed through theory and experiment that such high-frequency vibrations above 15 kHz can solve the problem of drilling difficult materials to some extent. As early as the twentieth century, Kumabe(5) discovered that this technology has a relatively excellent process effect because the cutting edge is periodically separated from the workpiece during machining, and there is also a static effect (displacement does not change with time) and rigidity effect of the drill bit (the pulse force improves the drill's ability to resist bending deformation). Zhang and Wang (18) also made significant contributions to the machining mechanism by experimentally demonstrating that vibratory drilling can also result in local chip breakage under certain conditions in zero phase difference and its neighborhood. The study by Brehl and Dow (3) helped to explain the basic kinematic relationships of vibratory tool trajectories and described how intermittent cutting mechanisms can reduce machining temperatures and extend tool life. Ma (8) explained the variable speed cutting, variable thickness cutting, variable angle cutting and separation impact characteristics of the vibratory drilling process. In terms of applied research, Mikhailova et al. (9) applied ultrasound-assisted technology to marble drilling, and found to reduce part damage due to machining. Baraheni and Amini (1) applied it to drilling of glass fiber reinforced plastics, and studied and improved drilling parameters. Shao et al. (11) applied it to carbon fiber composite material drilling and found that it can effectively improve the processing quality of drilling. MA et al. (7) also applied ultrasound-assisted technology to the processing of carbon fiber composites and investigated the effect of load on tool vibration amplitude. All these studies proved that ultrasonic-assisted drilling technology can improve the quality of drilling. Other scholars have taken another approach, Yuan et al. (16) placed the ultrasonic vibration process after machining and used a tool head loaded with ultrasonic vibration to remove the burrs generated in deep holes, blind holes, cross holes and other machining locations. Liu et al. (6), on the other hand, used electrolytic rotary ultrasonic-magnetic composite machining technique to remove burrs from the hole edges of TC4 titanium alloy, and the hole roughness was also significantly reduced. It can be seen that ultrasonic-assisted drilling in a single material and common size hole processing has a strong research base, but the field of PCB processing has a special nature, micro-hole, composite materials, size effect on ultrasonic-assisted processing brought about by the impact of all need further research.

The non-polar resin, flat glass fiber, and multiple and hard fillers used in high-speed circuit boards have all led to micro-hole processing becoming more difficult. Therefore, this paper conducts a study with the aim

of improving the micro-hole quality of high-speed circuit boards, and proposes a new processing method for the poor micro-hole drilling quality of high-speed circuit boards by applying ultrasonic-assisted drilling technology to PCB micro-hole processing. The specific research includes the mechanistic study and experimental study of ultrasonic-assisted drilling of high-speed circuit boards to obtain the influence mechanism of each processing parameter on the quality of micro-hole processing and provide theoretical guidance for the actual processing of high-speed circuit boards.

2. Ultrasonic-assisted Drilling Mechanism Studies

2.1 Study on the tool trajectory variation of ultrasonic-assisted drilling

The principle of ultrasonic-assisted drilling is to load high-frequency ultrasonic vibration vibrations on the drill or workpiece, so that the drilling process becomes a compound motion of high-speed rotary motion of the drill, feed motion and ultrasonic high-frequency vibration. Therefore, this paper takes the trajectory change of micro-drilling as the entry point for in-depth study by establishing the motion model of the tool.

A point on the micro-drill blade is selected as the object for analysis, and the displacement of the point in the z-direction relative to the workpiece after adding the ultrasonic vibration term to the conventional model is:

$$z = f_r nt + A\sin 2\pi ft$$

1

where: *fr* is the feed rate (mm/r), *n* is the micro-drilling speed (r/min); *A* is the ultrasonic amplitude (mm), *f* is the ultrasonic vibration frequency (Hz).

Let the angular velocity of the micro-drill's own rotational motion during ultrasonic vibration drilling be ω (rad/s), then the relationship between the angular velocity and time *t* is:

$$t = \frac{\theta}{\omega} = \frac{\theta}{2\pi n/60} = \frac{30\theta}{\pi n}$$

2

where: θ is the angular displacement (rad).

After eliminating the time t by coupling (1) and (2), the expression for the displacement *z* of the analyzed point on the tool with respect to the workpiece becomes:

$$z = \frac{30\theta f_r}{\pi} + A\sin\frac{60\theta f}{n}$$

3

By expanding the coordinates of the analyzed points in a three-dimensional coordinate system, the equation of the trajectory of a point on the micro-drill blade is finally obtained:

$$\begin{cases} x = r\cos\theta \\ y = r\sin\theta \\ z = \frac{30\theta f_r}{\pi} + A\sin\frac{60\theta f}{n} \end{cases}$$

4

where: r is the micro-drilling radius (mm).

After substituting r = 0.15mm, the Eq. (4) is plotted in MATLBA, and the trajectory diagram of the analysis point relative to the workpiece during ultrasonic-assisted drilling can be obtained, and similarly the trajectory diagram of the point during ordinary drilling can be obtained by removing the ultrasonic term, and a comparison of the two is shown in Fig. 3. It can be seen that the cutting path of the tool during ultrasonic vibration-assisted drilling is not a monotonic curve as in ordinary drilling, and the tool is not pressed against the workpiece and fed all the time, but does axial reciprocating motion with high frequency.

Combined with the structural analysis of the micro-drill, it is known that within the microscopic scale, the main cutting edge and the cross-edge of the drill are in contact and then separated from the workpiece periodically all the time, cutting with a pulsating separation intermittent motion. This tiny amplitude vibration impact strengthens the cutting ability of the main cutting edge and cross-edge, especially the cross-edge which will only press the workpiece tightly during ordinary drilling, and after loading ultrasonic vibration, it will continuously impact the part of the material that is not removed, and with the high speed rotation of the micro-drill also plays a role in drilling, which eventually makes the material removal easier. On the other hand, the sub-cutting edge of the micro-drill also scrapes the hole wall reciprocally all the time because of the high-frequency axial vibration, and plays a plowing role under the high-speed rotation, which is equivalent to the secondary processing of the hole wall, which has a positive impact on the improvement of micro-hole quality.

2.2 Study on the variation of effective cutting angle of ultrasonic-assisted drilling tools

The loading of ultrasonic vibration also has an effect on the effective cutting angle of the tool. If the ultrasonic vibration drilling tool trajectory obtained in Fig. 3 is expanded laterally, the sine curve shown in Fig. 4 can be obtained, and it can be seen that the effective front angle α and effective back angle γ of the tool change with the tool trajectory during ultrasonic-assisted drilling. Figures 4 represent the tool cutting the workpiece at different angles with ultrasonic vibration. In one vibration cycle, the effective front angle α of the micro-drill cutting edge increases and then decreases in the cutting-in phase (when moving in the

feed direction) until it is the same as that in ordinary cutting, and then decreases and then increases in the cutting-out phase (when moving in the opposite direction from the feed) before finally entering the next cycle; while the change trend of the effective rear angle γ is always opposite to the effective front angle. In contrast, the trajectory of the main cutting edge in ordinary drilling can be regarded as a straight line in a certain time, and the front and rear angles of the tool do not change.

According to the M.E. Merchant cutting equation, the formula for the shear angle can be obtained by the principle of minimum combined force:

$$\phi = \frac{\pi}{4} - \frac{\beta}{2} + \frac{\alpha}{2}$$

5

And the degree of deformation of the workpiece material during cutting can be measured by the relative slip ε and the deformation coefficient ξ. As shown in Fig. 5, when the cut material is squeezed and slid to OM by the tool, the distance of shear surface slip should be △y. Considering that the value of △y is very small when micro cutting, it can be considered that the material slip occurs on the shear surface, then the slip amount should be △s.

The relative slip ε is mainly used to reflect the degree of slip deformation in the deformed zone during cutting, and the deformation coefficient ξ is mainly used to measure the change in the generated chip geometry. The expressions of both are:

$$\varepsilon = \frac{\Delta s}{\Delta y} = \cot\phi + \tan(\phi - \alpha)$$

6

$$\xi = \frac{h_c}{h_0} = \frac{OM\cos(\phi - \alpha)}{OM\sin\phi} = \cot\phi\cos\alpha + \sin\alpha$$

7

Combined with the analysis of Fig. 4, Eq. (5), Eq. (6) and Eq. (7), it can be seen that when the micro-drill vibrates toward the feeding direction, the increase of the effective front angle α leads to the increase of the shear angle φ, and the increase of both makes the relative slip ε and the deformation coefficient ξ decrease, i.e., the deformation and friction of the cut material by extrusion are reduced, and the chips are more easily discharged by flowing into the spiral groove along the cutting edge, which finally leads to the reduction of the cutting force of ultrasonic-assisted drilling. And when the micro-drill vibrates in the direction opposite to the feeding direction, although the effective front angle α increases at this time, the micro-drill cutting edge is in the cut-out stage, gradually moving away from the workpiece material, and the material being cut keeps decreasing, even stopping the machining with empty cutting in a relatively short period of time. This law of change in the effective angle of the tool, coupled with the fact that the

micro-drilling cutting edge is cutting in a pulsed separation intermittent motion, makes ultrasonic-assisted drilling technology conducive to the reduction of the average drilling force and drilling temperature.

In summary, the reduced deformation of the material being cut during ultrasonic-assisted drilling results in reduction in drilling force and temperature and a smoother material removal process, which has a very positive impact on the quality of micro-hole drilling.

2.3 Study on the chip thickness variation of ultrasonic-assisted drilling

Continuing the analysis on the basis of the tool motion model in the previous section, chip generation and fracture can also be studied. The micro-drill used for PCB micro-hole machining in this study makes a double-edged, all the expression of the displacement of the analysis point in Eq. (3) is written as Z_1, then in symmetrically selected analysis point on the other edge, the displacement of which is written as Z_2, the expression is:

$$z_2 = \frac{30(\theta + \pi)f_r}{\pi} + A\sin\frac{60(\theta + \pi)f}{n}$$

8

So in ultrasonic vibration drilling, the two edges of the tool are alternately cutting the workpiece, then it can be deduced that the cutting thickness during processing should be:

$$t_d = z_2 - z_1 = 30f_r + 2A\cos\frac{30(2\theta + \pi)f}{n}\sin\frac{30\pi f}{n}$$

9

The size of the chip thickness determines whether the chip can be generated or not. When the chip thickness becomes zero or even negative, it indicates that geometrically the trajectories of the two edges of the micro-drill are intersecting and the chip is fractured.

As shown in the Fig. 6, the dynamic axial cutting thickness curve is drawn according to Eq. (9). According to the previous section, in a certain time, the trajectory of the main cutting edge can be regarded as a straight line during ordinary drilling, so its cutting thickness will not change, and the material to be cut will move along the spiral groove of the micro-drill for a certain distance before fracture occurs, so the long spiral type chips will account for a large part of ordinary drilling. However, the cutting thickness changes dynamically during ultrasonic-assisted drilling, and there will be both mechanical chip breakage and geometric chip breakage in the actual processing, and the proportion of short spiral type, ribbon type and broken block type in the chips will increase significantly. Moreover, as the drilling depth increases, the long spiral type chips appearing in ordinary drilling will be subject to the joint action of the front tool surface of the micro-drill, the inner wall of the spiral groove and the hole wall, and may be bent and folded due to extrusion, which is more unfavorable to discharge out of the hole, and even blockage of the hole will occur; on the contrary, ultrasonic-assisted drilling is not only favorable to the improvement of the chip

breaking ability, but also easier to generate and discharge more easily banded and broken type chips, which will have a positive impact on the chip discharge, which improve the chip removal ability and reduces the risk of plugging.

3. Materials And Methods Of Ultrasonic-assisted Drilling Experiment

3.1 Experimental materials and apparatus

The drill bit selected in this study is a double-edged, single-groove micro-drill with a diameter of 0.3 mm, and the specific structural parameters are shown in the table below.

Table 1
Experimental micro-drill structure parameters.

Diameter (mm)	Point angle (°)	Helix angle (°)	Web thickness (mm)	Flute length (mm)	Full length (mm)	Gutter width ratio
0.30	120	40	0.16mm	6.5	38.1	1:2

There are two kinds of PCBs selected in the study, among which the lead-free and halogen-free medium Tg circuit board is used in the single-factor experiment; the high-speed board S1000 is used in the orthogonal experiment, whose dielectric loss Df value is 0.009 and belongs to the medium Tg, low Z-axis thermal expansion coefficient board, and the main components are copper foil, glass fiber and brominated epoxy resin combination, etc.

The ultrasonic-assisted drilling experimental platform used in this experiment is designed and built based on the existing single-axis vertical drilling machine for PCB drilling, and its structural design is shown in Fig. 7. The experimental platform as a whole is placed under the pneumatic spindle and consists of three parts: the bakelite plate at the bottom, the ultrasonic vibration plate and the ultrasonic transducer. The bottom bakelite plate is completely fixed with the marble table of the machine tool as the base plate; the ultrasonic vibration plate plays the role of bearing the workpiece and conducting vibration, which is fixed in the rectangular groove of the bakelite plate by a large number of small tabs, and is not locked with bolts to ensure its vibration performance, and only restricts its movement in the plane, and the vibration in the vertical direction is not constrained; the ultrasonic transducer is welded on the middle line of the ultrasonic vibration plate, and leads to the wire The ultrasonic transducer is welded to the center line of the ultrasonic vibration plate, and leads to the wire connected to the external 20kHz automatic frequency sweep type ultrasonic generator of the machine tool, the role of these two is to generate ultrasonic signals and converted into mechanical vibration.

After the experimental platform was built, the amplitude of the loaded vibration plate was also measured, and the actual amplitude of the workpiece at different power levels is shown in the Table 2.

Table 2
Workpiece amplitude at different ultrasonic generator power levels.

Ultrasonic power	0	15%	25%	35%	45%
Amplitude (μm)	0	1.4708	1.5763	1.7128	2.3338

3.2 Experimental methods

The specific flow of the experiment is shown in the Fig. 8:

Figure 8(a) shows the physical ultrasonic-assisted drilling experimental platform built, and Fig. 8(b) shows the external ultrasonic generator. After the drilling experiment of the printed circuit board on this platform, it is possible to take samples to make PCB micro slices, and the finished products are shown in Fig. 8(d).

The quality of micro-hole processing is evaluated by observing the images of PCB micro-slice collected through the ultra-deep field microscope in Fig. 8(e), and measuring and recording the micro-hole roughness, burr and nail head, and the morphology of the three defects in the ultra-deep field microscope is shown in Fig. 9(a), 9(b), 9(c) and 9(d).

The experiments in this study are divided into two parts as shown in Fig. 10: single-factor experiments and orthogonal experiments. The purpose of the single-factor experiments is to demonstrate the improvement effect of ultrasonic assistance on micro-hole processing quality and to provide more reasonable experimental factor levels for the subsequent orthogonal experiments. Then orthogonal experiments were conducted to study the significance level and the order of influence of each parameter on the microporous quality and to obtain a better combination of processing parameter levels.

The processing parameters used in the single-factor experiments are shown in the table below, and the initial parameters are selected from the parameter recommendation table of the micro-drill manufacturer.

Table 3
Parameters of the single-factor experiment for ultrasound effect validation.

Experimental factors	Level
Spindle speed (krpm)	110、145、170
Feed rate (mm/s)	28、34、41
Ultrasonic power	0、15%、25%、35%、45%

4. Results And Discussions

4.1 Single-factor experiment for ultrasound effect validation

The independent variable of the single-factor experiment for ultrasonic effect verification was ultrasonic intensity, but in order to prove the applicability of ultrasonic, three levels of feed rate were also used to repeat the experiment separately after fixing the spindle speed to 110 krpm, and the three sets of experiments were observed and analyzed separately. The experimental results were observed in an ultra-field depth microscope as shown in Fig. 11.

The single-factor experimental data for the ultrasonic effect validation were counted and plotted as two-dimensional line graphs of the results for micro-hole roughness, entrance burr, and exit burr, respectively. Figure 12 shows the results of the average micro-hole roughness measurements for the repeated experiments with three different drilling parameters.

It can be seen that the micro-hole roughness values show an overall decreasing trend after loading ultrasonic vibration at different drilling parameters, but at a certain level of ultrasonic intensity, the micro-hole roughness values at some of the parameters show a slight increase again. This is because the micro-hole roughness of the PCB is determined by the processing of the copper foil layer and the resin-glass fiber layer together. Copper foil is a plastic material, ultrasonic vibration not only enhances the cutting effect of the main cutting edge of the micro-drill on the copper foil material, it also causes the secondary cutting edge to rework the fracture of the copper foil material at the hole wall under high frequency reciprocal vibration, which makes the ductile fracture of the copper foil protruding from the hole wall occur again.

However, glass fiber composites with anisotropy will fracture in different ways depending on the angle between the cutting direction and the fiber direction. And when the amplitude of ultrasonic vibration increases to a certain level, the resin softened by the high temperature inside the hole will be deformed as the micro-drill pulls on the glass fiber supporting it, causing the micro-hole roughness to rise slightly. However, regardless of the ultrasonic intensity, the micro-hole roughness values are smaller under different drilling parameters than for ordinary drilling, which is sufficient to prove that the ultrasonic-assisted technology has an improved effect on the micro-hole quality of PCBs.

In addition to the micro-hole roughness, ultrasonic-assisted drilling has a good improvement on the burr generation. As Fig. 13 shows the average entrance burr length measurement results for the repeated experiments with three different drilling parameters.

The entrance burr is formed because the copper foil material at the edge of the hole is also squeezed during drilling, and the micro-drill moves the deformed material upwards a small distance when it is retired. Therefore, the burr is actually a plastic flow deformation of the copper foil material that has not been removed and turned into chips. From the previous mechanistic study, it is clear that the effective front-to-back angle of the cutting edge changes periodically during ultrasonic-assisted drilling, which reduces the force on the residual material in the direction of the workpiece when the cutting edge cuts into the workpiece and weakens the burr formation. In addition, the high-frequency vibration of the micro-drill in the feed direction causes the copper foil material at the edge of the hole at the entrance to be constantly scraped by the side of the micro-drill. The sub-cutting edge of the micro-drill also cuts the

material around the hole in the feed direction due to the high-frequency vibration in the axial direction when drilling and retracting the tool, which has the effect of smoothing the burr.

Figure 14 below shows a line graph of the average exit burr lengths measured from repeated experiments with three different drilling parameters.

The exit burr is also caused by the plastic flow deformation of the copper foil material, but for the exit part of the material, the contact time between the micro-drill blade and it is only for a short moment when it drills through and then immediately retires. Therefore, the scraping and plowing effect of the micro-drill on the exit burr is very limited, but the improvement effect due to the effective front angle and the change of the cutting thickness still exists, so it can still be seen that the exit burr length is smaller after loading ultrasound than when it is not loaded.

In summary, ultrasonic-assisted vibration drilling has improved the micro-hole roughness, entrance burr, and exit burr defects of printed circuit boards, proving the effectiveness of ultrasonic vibration drilling.

4.2 Orthogonal experiment of ultrasonic-assisted drilling of high-speed circuit board

Prior to the orthogonal experiments, single-factor experiments for parameter optimization were also conducted in this paper, and the parameters and results are shown in the following table.

Table 4
Micro-hole roughness and Entrance Burrs results of the single-factor experiments for optimization of ultrasonic processing parameters (25% ultrasonic power).

Number	Spindle speed (krpm)	Feed rate (mm/s)	Micro-hole roughness (μm)	Entrance Burrs (μm)
1	110	28	5.837	19.33
2	110	34	4.930	23.00
3	110	41	5.133	6.333
4	145	28	6.353	11.67
5	145	34	5.553	11.78
6	145	41	6.513	17.89
7	170	28	7.073	14.00
8	170	34	8.437	13.89
9	170	41	8.797	16.89

To facilitate comparison and get more intuitive analysis results, the data results of micro-hole roughness and entrance burr cases are plotted as the following surface plots to study respectively, and the surface

distribution is the data results in μm.

Analysis of Fig. 15 shows that although increasing the feed speed can also suppress the burr formation to some extent, this effect can be confused with the improvement of burr by ultrasonic vibration assistance, and increasing the feed speed also leads to a rise in hole roughness, so the range of feed speed is adjusted downward during parameter optimization. Analysis of Fig. 16 shows that the best value of micro-hole roughness occurs at a lower spindle speed, and the trend of the effect of speed on burr is not obvious in this group of experimental data, and the value of burr length fluctuates with the change of feed speed at a lower spindle speed.

The optimization results of the machining parameters under ultrasonic-assisted vibration drilling were obtained as shown in the Table 5.

Table 5
Parameters of orthogonal experiment of ultrasonic-assisted drilling of high-speed circuit board.

Experimental factors	Level
Spindle speed (krpm)	100、130、160
Feed rate (mm/s)	21、27、33
Ultrasonic power	0、25%、45%

Finally, an orthogonal test was performed based on this parameter. Since it was found that the ultrasonic-assisted technique also had an improvement effect on the generation of nail head (circuit board copper layer thickness of 30 μm) when drilling high-speed circuit boards, the nail head were also included in the evaluation criteria for micro-hole quality, and a three-index L9(33) orthogonal test was conducted, and the Table 6 was obtained after compiling the results.

Table 6
Orthogonal experiment results of ultrasonic-assisted drilling.

Number	Spindle speed (krpm)	Feed rate (mm/s)	Ultrasonic power	Micro-hole roughness (μm)	Entrance burrs (μm)	Nail head (μm)
1	100	21	0	9.785	17.14	50.67
2	100	27	25%	5.177	5.488	37.56
3	100	33	45%	4.737	10.11	41.26
4	130	21	25%	4.577	6.132	39.73
5	130	27	45%	5.196	12.12	43.85
6	130	33	0	12.40	15.70	53.82
7	160	21	45%	5.137	13.78	46.41
8	160	27	0	8.258	19.56	51.79
9	160	33	25%	5.236	7.408	41.39

First, the results of the orthogonal experiments were analyzed by polar difference analysis. The polar difference (R) indicates the magnitude of the change of the experimental index within the range of the value of the factor, and the larger the R value is, the greater the influence of the level change of the factor on the experimental index. The results of the analysis for microporous roughness, entrance burr and nail head are shown in Tables 7, 8 and 9, respectively.

Table 7
Micro-hole roughness polarization analysis for ultrasonic-assisted drilling orthogonal experiment.

Results	Spindle speed	Feed rate	Ultrasonic power
K1	19.699	19.499	30.443
K2	22.173	18.631	14.99
K3	18.631	22.373	15.07
k1	6.566	6.500	10.15
k2	7.391	6.210	4.997
k3	6.210	7.458	5.023
Range	1.181	1.248	5.153
Order of influence	Ultrasonic power > Feed rate > Spindle speed		
Optimal level	160krpm	27mm/s	25%
Optimal combination	$A_3B_2C_2$		

The results show that the most influential factor on the micro-hole roughness results is the ultrasonic power, and the feed rate and spindle speed have a similar influence. From the derived better levels of each factor, the lowest micro-hole roughness values can be obtained at spindle speed of 160 krpm, feed speed of 27 mm/s and ultrasonic intensity of 25%, i.e., when the feed speed is reduced to 27 mm/s during ultrasonic vibration, the high frequency vibration and feed motion of the micro-drill pulls less on the glass fiber inside the hole, and the ultrasonic plowing effect on it is very good, while the trend of the ultrasonic power part is similar to The results of the previous single-factor test are similar, too high ultrasonic power, that is, when the ultrasonic amplitude is too high instead of slightly reducing the hole wall quality, so loading 25% intensity of ultrasonic vibration can get the best results, reducing 50.8%.

Table 8
Entrance burrs polarization analysis for ultrasonic-assisted drilling orthogonal experiment.

Results	Spindle speed	Feed rate	Ultrasonic power
K1	32.738	37.082	52.40
K2	33.952	37.28	19.028
K3	40.748	33.218	36.01
k1	10.91	12.36	17.47
k2	11.32	12.39	6.343
k3	13.58	11.07	12.00
Range	2.67	1.32	11.127
Order of influence	Ultrasonic power > Spindle speed > Feed rate		
Optimal level	100krpm	33mm/s	25%
Optimal combination	$A_1B_3C_2$		

The results show that the most influential factor on the entrance burr length is still the ultrasonic power, followed by the spindle speed. From the derived better levels of each factor, the smallest entrance burr length is obtained at spindle speed of 100 krpm, feed rate of 33 mm/s and ultrasonic intensity of 25%. The trend in the spindle speed and feed rate sections is not quite the same as the micro-hole roughness because the entrance burr is mainly formed by the flow plastic deformation of the copper foil material at the edge of the hole, while the micro-hole roughness is determined by the processing condition of the material inside the hole. The higher feed rate affects the processing quality of the material inside the hole, but the copper foil at the orifice still has a better processing quality under ultrasonic vibration. The ultrasonic power also gives the smallest burr length at 25%, but in fact, it can be seen from the calculated ki value that the difference between 25% level and 45% level is only 7.2%, while the difference with and without ultrasonic loading is 47.1%, which is enough to prove the improvement effect of ultrasonic vibration loading on the entrance burr.

Table 9
Nail head polarization analysis for ultrasonic-assisted drilling orthogonal experiment.

Results	Spindle speed	Feed rate	Ultrasonic power
K1	129.49	136.81	156.28
K2	137.4	133.2	118.68
K3	139.59	136.47	131.52
k1	43.16	45.60	52.09
k2	45.8	44.4	39.56
k3	46.53	45.49	43.84
Range	3.37	1.2	12.53
Order of influence	Ultrasonic power > Spindle speed > Feed rate		
Optimal level	100krpm	27mm/s	25%
Optimal combination	$A_1B_2C_2$		

The results show that the most influential factor on the nail head length remains the ultrasonic power, followed by the spindle speed. From the resulting optimal level of each factor, the smallest nail head length was obtained at a spindle speed of 100 krpm, a feed rate of 27 mm/s, and an ultrasonic intensity of 25%. This is because the nail head is actually a flow plastic deformation of the copper foil layer material, but it occurs in the hole, and the principle of its generation is very similar to that of the entrance burr, and the ultrasonic vibration loading has a similar principle of their improvement. The improvement effect of the spindle speed is still very obvious.

Table 10
Comparison of the impact of factors for each indicator.

Parameter	Order of influence	Optimal combination
Micro-hole roughness	Ultrasonic power > Feed rate > Spindle speed	$A_3B_2C_2$
Entrance burrs	Ultrasonic power > Spindle speed > Feed rate	$A_1B_3C_2$
Nail head	Ultrasonic power > Spindle speed > Feed rate	$A_1B_2C_2$

Since the optimal combinations obtained from the extreme difference analysis of the three influencing factors are not exactly the same, they also need to be judged by comparing the order of their influences. As shown in Table 10, there is no doubt that the ultrasonic power (factor C) has the greatest influence, with a better level of 25% for both. The spindle speed (factor A), which has the second influence on both the entrance burr and the nail head, is only 5.7% different from the feed speed and spindle speed as

calculated in the micro-hole roughness extreme difference analysis, so the spindle speed is taken as the second criterion in the combination of the better process parameters, and the first level, i.e. 100krpm, is selected as the best value for both the entrance burr and the nail head. It can be concluded that the best combination of parameters for ultrasonic vibration-assisted drilling to obtain the best overall drilling quality is spindle speed of 100 krpm, feed rate of 27 mm/s and ultrasonic intensity of 25%.

In addition, the effect of ultrasonic vibration assisted drilling can also be demonstrated by the change of chip morphology, combined with the conclusion obtained in the previous theoretical study of ultrasonic-assisted drilling process: ultrasonic vibration increases the proportion of short continuous chips, ribbon chips and broken chips in the chips, as shown in Fig. 17, which leads to the improvement of material removal and chip discharge in the hole, which is finally reflected in the processing quality of micro-hole. quality.

Then, the results of the orthogonal experiments were also analyzed by ANOVA, and the results of the analysis of the three influencing factors were tallied into the ANOVA table shown below.

Table 11
ANOVA of Micro-hole roughness during ultrasonic-assisted drilling.

Parameter	Sum of square	Degree of freedom	Meansquare	F	Fa	Significance level
Spindle speed	2.202	2	1.101	0.499	F0.5(2,2) = 1	
Feed rate	2.558	2	1.279	0.580	F0.5(2,2) = 1	
Ultrasonic power	52.796	2	26.398	11.975	F0.1(2,2) = 9	*
Residual	4.409	2	2.34			

Table 12
ANOVA of entrance burrs during ultrasonic-assisted drilling.

Parameter	Sum of square	Degree of freedom	Meansquare	F	Fa	Significance level
Spindle speed	12.414	2	6.207	25.831	F0.05(2,2) = 19	**
Feed rate	3.360	2	1.680	6.991	F0.5(2,2) = 1	*
Ultrasonic power	185.591	2	92.796	386.167	F0.01(2,2) = 99	***
Residual	0.481	2	0.240			

Table 13
ANOVA of Nail head during ultrasonic-assisted drilling.

Parameter	Sum of square	Degree of freedom	Meansquare	F	Fa	Significance level
Spindle speed	18.886	2	9.443	4.436	F0.5(2,2) = 1	*
Feed rate	2.647	2	1.323	0.622	F0.5(2,2) = 1	
Ultrasonic power	243.581	2	121.790	57.214	F0.05(2,2) = 19	**
Residual	4.257	2	2.129			

According to the analysis of the results of the significance test, after excluding the influence caused by random errors, the significant level of ultrasonic intensity is still the highest, and all three ANOVAs show that ultrasonic intensity has a significant effect on the machining quality of micro-hole, while the significance of spindle speed ranks second and the significance level of feed speed is lower, but all three have an effect on machining quality, and the most obvious effect on the entrance burr situation.

In summary, the ultrasonic assisted technology has very obvious improvement on several machining defects such as micro-hole roughness, entrance burr and nail head cases, and they have the same effect when the ultrasonic intensity is changed, and the spindle speed and feed rate have less obvious effect on machining quality than the ultrasonic power, but still a better combination of parameters can be obtained by extreme difference analysis. More importantly, the research method is not only applicable to PCBs in experiments, but provides a way to obtain the primary and secondary order and optimal level combinations of the effects of each parameter on the quality of micro-hole.

5. Conclusions

In this paper, a new ultrasonic-assisted drilling of high-speed circuit boards is proposed for the challenges of micro-hole quality of high-speed circuit boards. The impact mechanism of ultrasonic assist on the drilling method, material deformation, drilling force, chip breaking and chip removal of high-speed circuit boards is analyzed through the tool motion model. Then, the ultrasonic assisted drilling experimental platform is designed and built to carry out experiments on ultrasonic effect verification, drilling parameter optimization, and optimal parameter level combination analysis, and the following conclusions are obtained.

(1) The major difference between ordinary drilling and ultrasonic drilling is the difference in tool trajectory, the main cutting edge and cross edge of micro-drill are cutting with pulsed separation intermittent motion during ultrasonic-assisted drilling, and the secondary cutting edge is scraping the hole wall reciprocally, which improve the cutting ability of micro-drill and the quality of micro-hole.

(2) The effective cutting angle and cutting thickness of the ultrasonic-assisted drilling tool will change periodically, resulting in a reduction of the deformation of the processed material, which is conducive to the reduction of drilling force and temperature, and has a positive impact on chip breaking and chip removal, ultimately contributing to the improvement of micro-hole quality.

(3) Ultrasonic vibration loading on high-speed circuit board micro-hole roughness, entrance burr, nail head these kinds of processing defects of the situation have very obvious improvement, too high ultrasonic power will lead to a small decline in the quality of micro-hole processing, but compared to ordinary drilling of micro-hole quality or a relatively obvious improvement.

(4) When ultrasonic-assisted drilling of S1000 printed circuit boards, a better combination of parameters is spindle speed of 100 krpm, feed rate of 27 mm/s, and ultrasonic intensity of 25%. At the same time, a method that can obtain the primary and secondary order and the optimal level combination of the influence of each parameter on the micro-hole quality is provided, and the mechanism of the influence of micro-hole quality of ultrasonic-assisted drilling of PCBs is investigated in a comprehensive theoretical and experimental way, which provides a theoretical research basis and processing guidance for high-speed circuit board drilling.

Declarations

Acknowledgments

This research is supported by the National Natural Science Foundation of China (Nos. 51971150 and 52075344), the Natural Science Foundation of Guangdong Province (No. 2016A030310036), the Science and Technology Innovation Commission Shenzhen (Nos. JCYJ20170817101008562 and JSGG20190219152602381), and the Natural Science Foundation of Shenzhen University (No. 2017034).

-Ethical Approval

There were no ethical issues involved.

-Consent to Participate

There were no participants in this study.

-Consent to Publish

The authors agree to publication in the Journal. The copyright to the article is transferred to the publisher if and when the article is accepted for publication. The authors warrant that contribution is original and that the authors have full power to make this grant. The copyright transfer covers exclusive right to reproduce and distribute the article, including reprints, translations, photographic reproductions, microform, electronic form or any other reproductions of similar nature. After submission of the

agreement signed by the corresponding author, changes of authorship or in the order of the authors listed will be accepted by the publisher.

-Authors Contributions

Zhisen Gao contributed to establishe ultrasonic-assisted drilling tool motion model;

Hongyan Shi contributed to the conception of the study and wrote the manuscript;

Sha Tao contributed experiment plat and single-factor experiment for ultrasound effect ;

Xianwen Liu performed the orthogonal experiment of ultrasonic-assisted drilling;
Tao Zhu performed the data analyses ;

Zhuangpei Chen performed the experiment and manuscript preparation.

-Funding

The research is supported by the National Key Research and Development Program of China (No. 2020YFB1708500), the National Natural Science Foundation of China (No. 52075344), and the Science and Technology Innovation Commission Shenzhen (Nos. JSGG2019152602381 and JSGG20200914113603008).

-Competing Interests

All authors certify that they have no affiliations with or involvement in any organization or entity with any financial interest or non-financial interest in the subject matter or materials discussed in this manuscript.

-Availability of data and materials

All data generated or analysed during this study are included in this published article

References

1. Baraheni M, Amini S (2018) Feasibility study of delamination in rotary ultrasonic-assisted drilling of glass fiber reinforced plastics. J Reinf Plast Compos 37:3–12
2. Bhandari B, Hong YS, Yoon HS, Moon JS, Pham MQ, Lee GB, Huang YC, Linke BS, Dornfeld DA, Ahn SH (2014) Development of a micro-drilling burr-control chart for PCB drilling. Precis Eng 38:221–229
3. Brehl DE, Dow TA (2008) Review of vibration-assisted machining. Precision Engineering-Journal Of the International Societies for Precision Engineering And Nanotechnology 32:153–172
4. Ko SL, Chang JE, Yang GE (2003) Burr minimizing scheme in drilling. J Mater Process Technol 140:237–242

5. Kumabe J (1985) Precision Machining Vibratory Cutting: Fundamentals and Applications. Machinery Industry Press, Beijing
6. Liu XL, Chen Y, Wang J, Zhang GF (2019) Deburring of TC4 titanium alloy hole edge by magnetic grinding in combination with electrolysis and rotational ultrasonic vibration. Electroplating & Finishing | Electroplat Finish, pp 680–684
7. MA GF, Kang RK, Dong ZG (2020) Hole quality in longitudinal-torsional coupled ultrasonic vibration assisted drilling of carbon fiber reinforced plastics. Front Mech Eng 15:538–546
8. Ma LJ (2007) Experimental study on the mechanism of axial vibration drilling and its process effect. Jiangsu University, Jiangsu, pp 1–20
9. Mikhailova N, Onawumi PY, Volkov G, Smirnov I, Broseghini M, Roy A, Petrov Y, Silberschmidt VV (2019) Ultrasonically assisted drilling in marble.Journal Of Sound And Vibration460
10. Sahoo S, Thakur A, Gangopadhyay S (2016) Application of Analytical Simulation on Various Characteristics of Hole Quality during Micro-Drilling of Printed Circuit Board. Mater Manuf Processes 31:1927–1934
11. Shao Z, Jiang X, Geng D, Liu Y, Zheng W (2021) The interface temperature and its influence on surface integrity in ultrasonic-assisted drilling of CFRP/Ti stacks. Composite Structures, p 113803
12. Shi HY, Liu XW, Lou Y (2019) Materials and micro drilling of high frequency and high speed printed circuit board: a review. Int J Adv Manuf Technol 100:827–841
13. Song YX, Fu LY, Zheng LJ, Yang LP, Wang CY (2012) Characteristics of chip formation in the micro-drilling of multi-material sheets. Int J Mach Tools Manufacture: Des Res application 52:40–49
14. Wang YS, Zou B, Yin GG (2019) Wear mechanisms of Ti(C7N3)-based cermet micro-drill and machining quality during ultra-high speed micro-drilling multi-layered PCB consisting of copper foil and glass fiber reinforced plastics. Ceram Int 45:24578–24593
15. Watanabe H, Tsuzaka H, Masuda M (2008) Microdrilling for printed circuit boards (PCBs)—Influence of radial run-out of microdrills on hole quality. Precis Eng 32:329–335
16. Yuan YJ, Wei ZL, Fu B (2020) Design and vibration characteristics analysis of ultrasonic vibration deburring tool head. Mechanical Engineer, pp 22–24
17. Zhang CX, Zhang WF, Liu ZJ, Zhang FX (2021) Research status and development trend of rotary ultrasonic drilling process. Mach Building Autom 50:1–5
18. Zhang DY, Wang LJ (1993) Local chip breaking characteristics of vibratory drilling.Journal of Applied Sciences,337–344
19. Zhang Y, Kang RK, Liu JT, Zhang YM, Zheng WS, Dong ZG (2017) Review of ultrasonic vibration-assisted drilling technology. J Mech Eng 53:33–44
20. Zhu DT (2019) Discussion on the development of high-speed laminate technology, Proceedings of the 20th China Copper Clad Technology Symposium, Suzhou, Jiangsu, China, p. 15

Figures

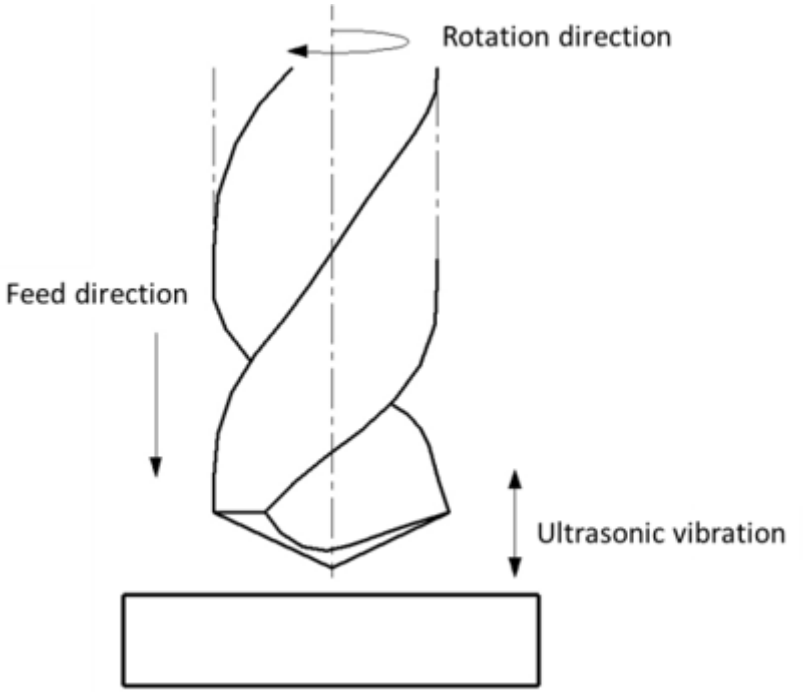

Figure 1

Ultrasonic-assisted drilling motion model.

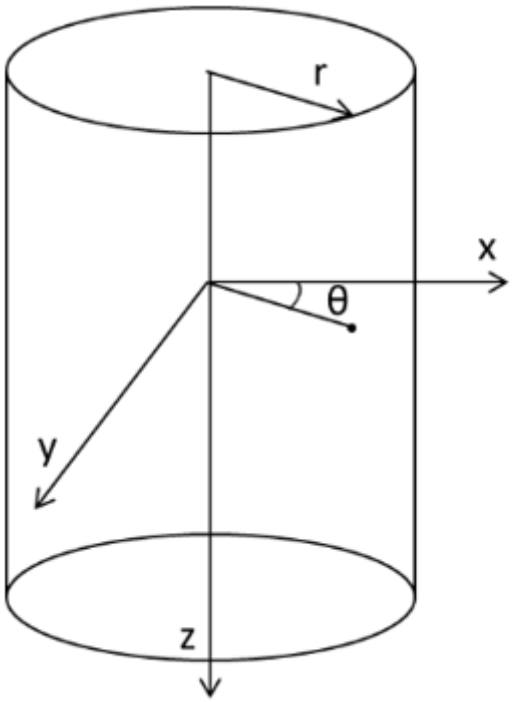

Figure 2

Analysis points are expanded in a three-dimensional coordinate system.

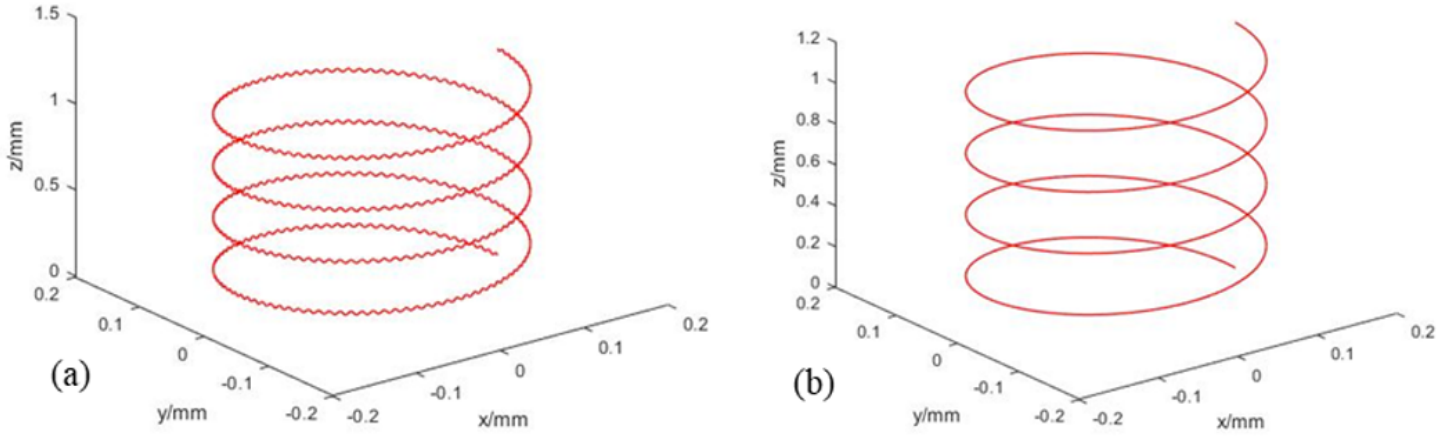

Figure 3

Comparison of tool trajectory between ultrasonic-assisted drilling (a) and normal drilling (b).

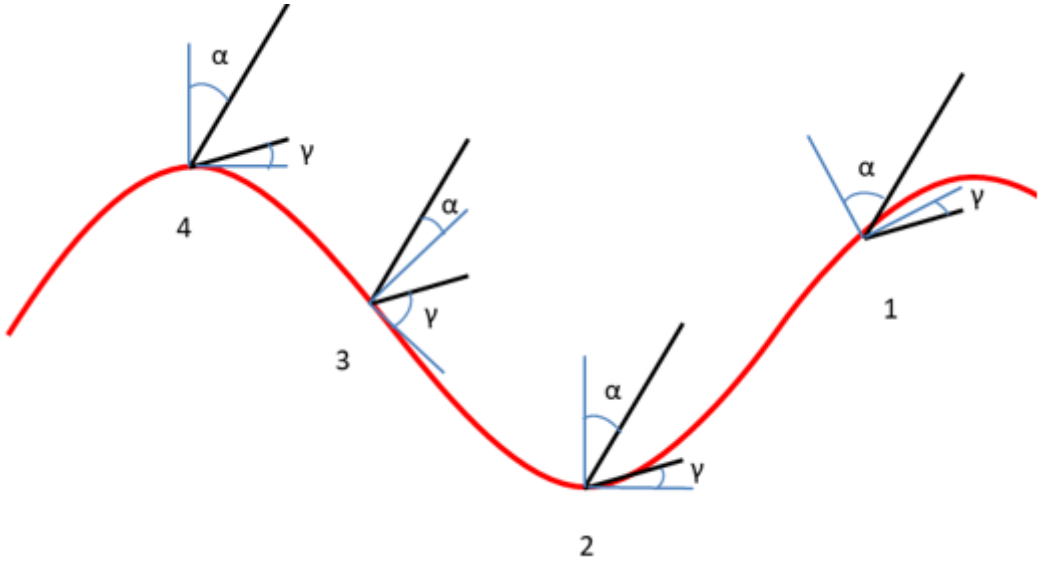

Figure 4

Trend of effective cutting angle of tool during ultrasonic assisted drilling.

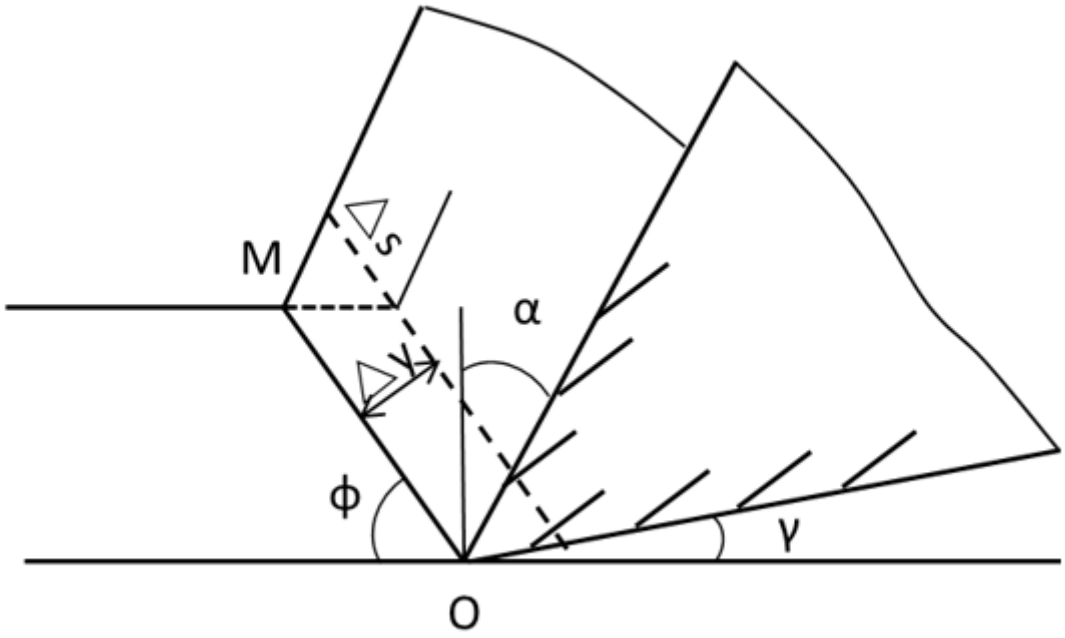

Figure 5

Micro-cutting diagram.

Figure 6

Dynamic axial cutting thickness.

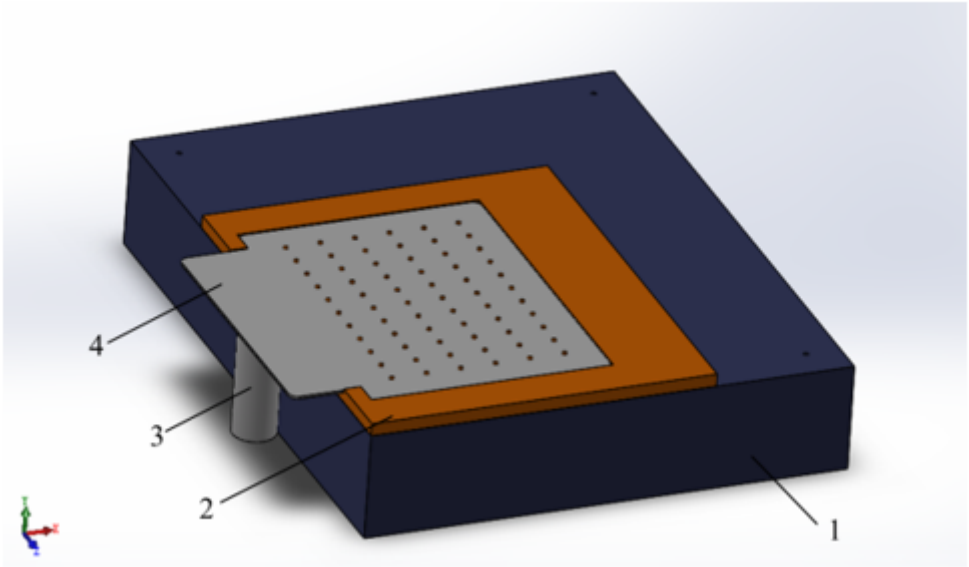

Figure 7

Ultrasonic vibration platform: (1)Marble; (2)Bakelite board; (3)Ultrasonic transducer; (4) Ultrasonic vibration plate.

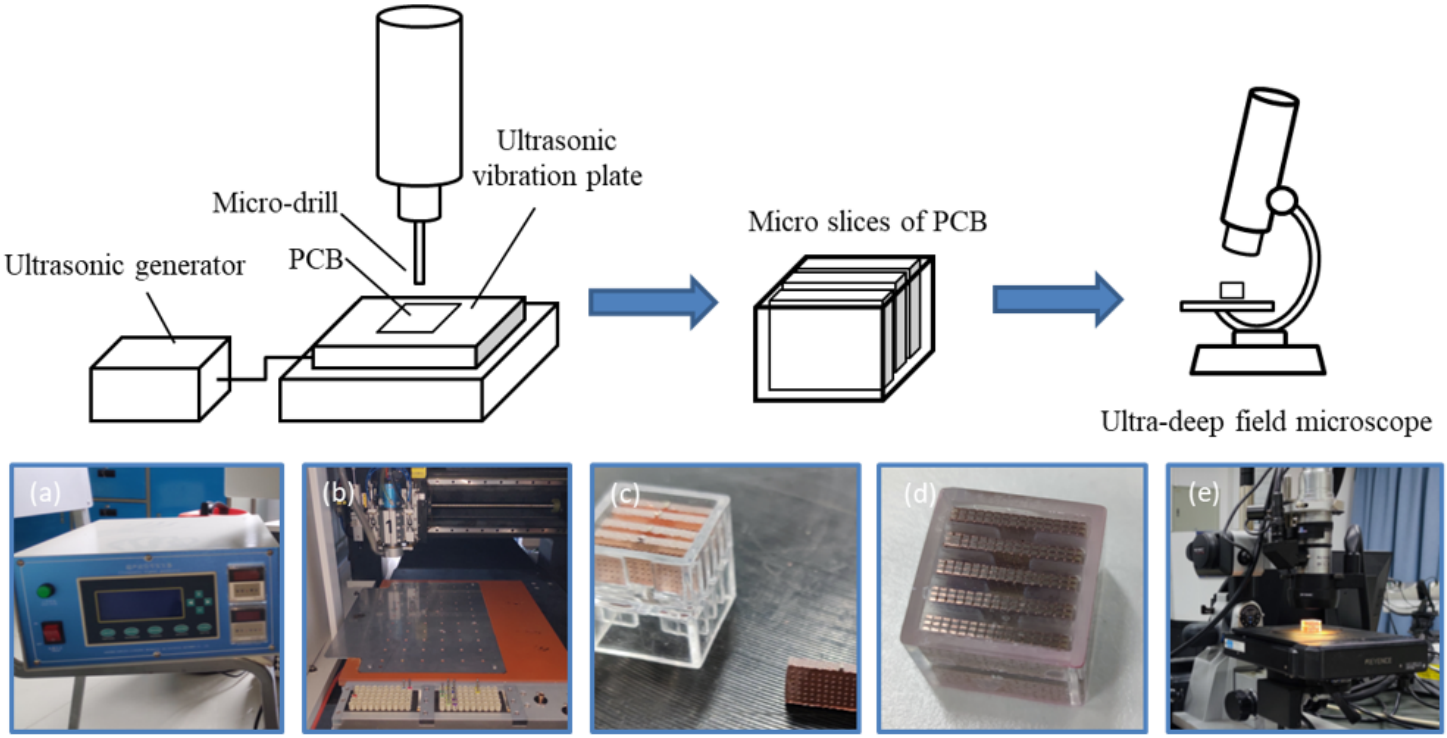

Figure 8

Schematic diagram of the experimental methods: (a)Ultrasonic generator; (b)Ultrasonic vibration plate; (c-d) Micro slices of PCB; (e) Ultra-deep field microscope.

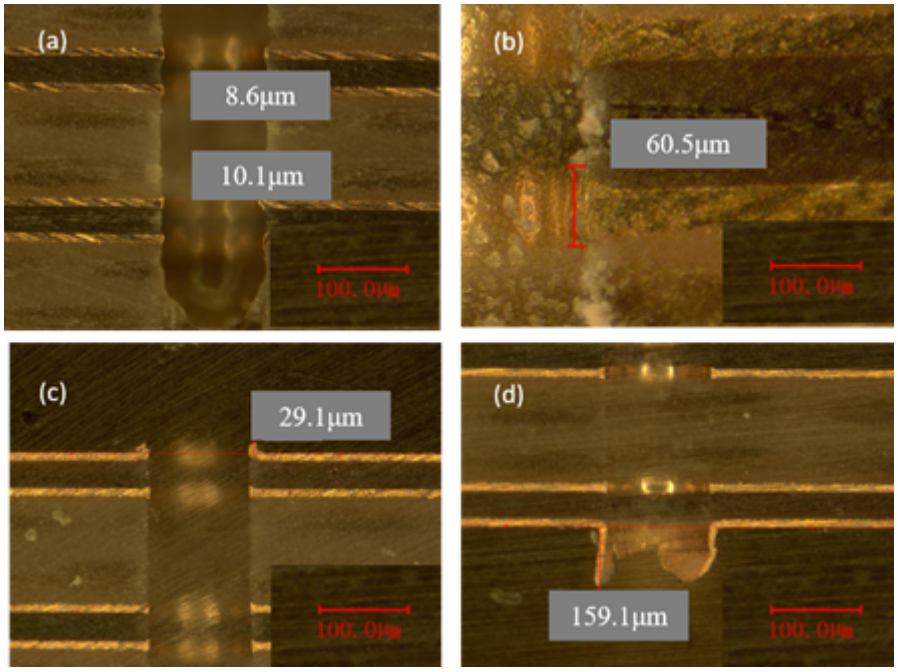

Figure 9

Micro-hole processing defects: (a) micro-hole roughness; (b) nail head; (c) entrance burr; (d) exit burr.

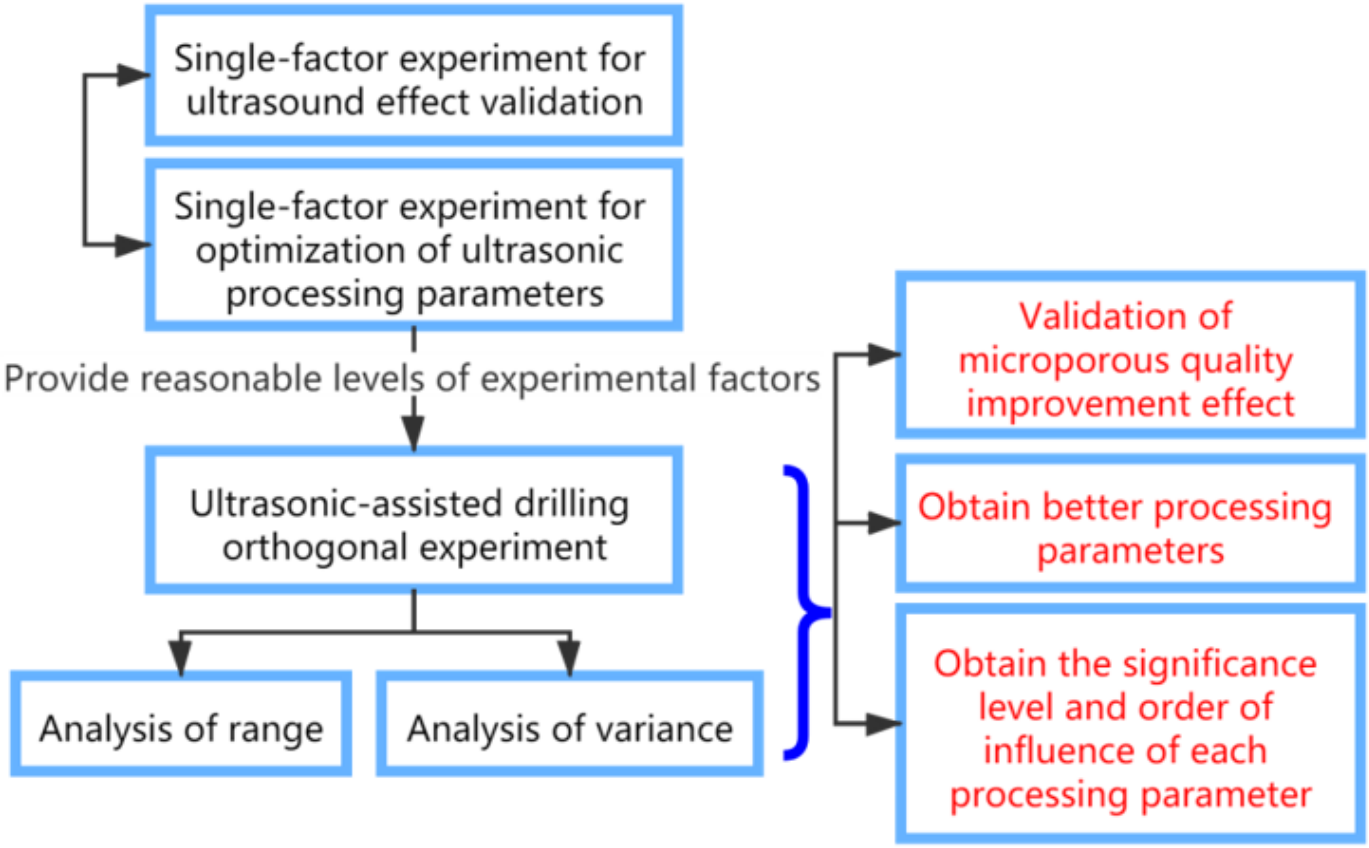

Figure 10

Flow chart of the experiment.

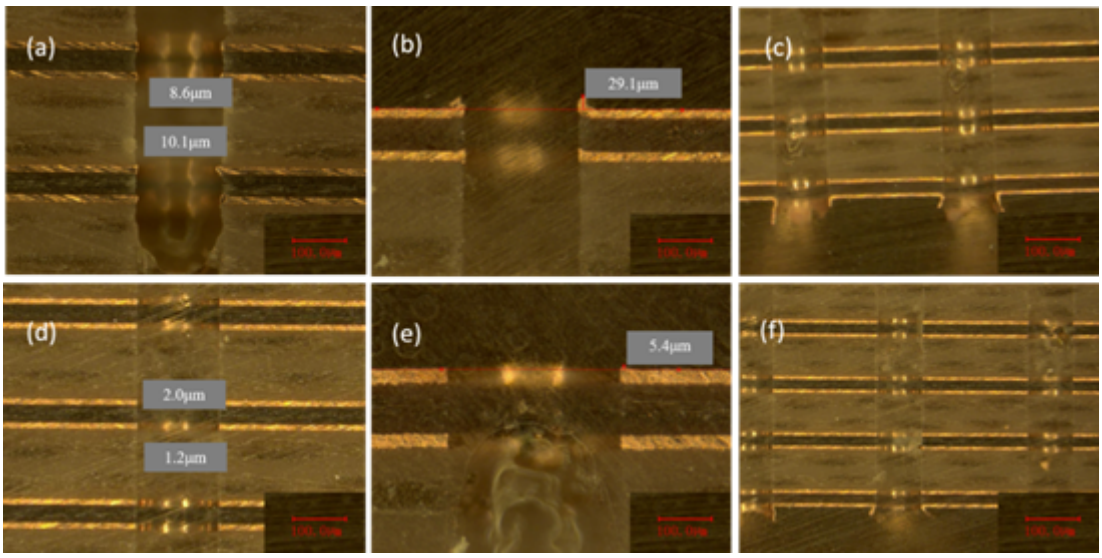

Figure 11

Example of single-factor experimental results normal drilling (a) (b) (c) and ultrasonic-assisted drilling (d) (e) (f).

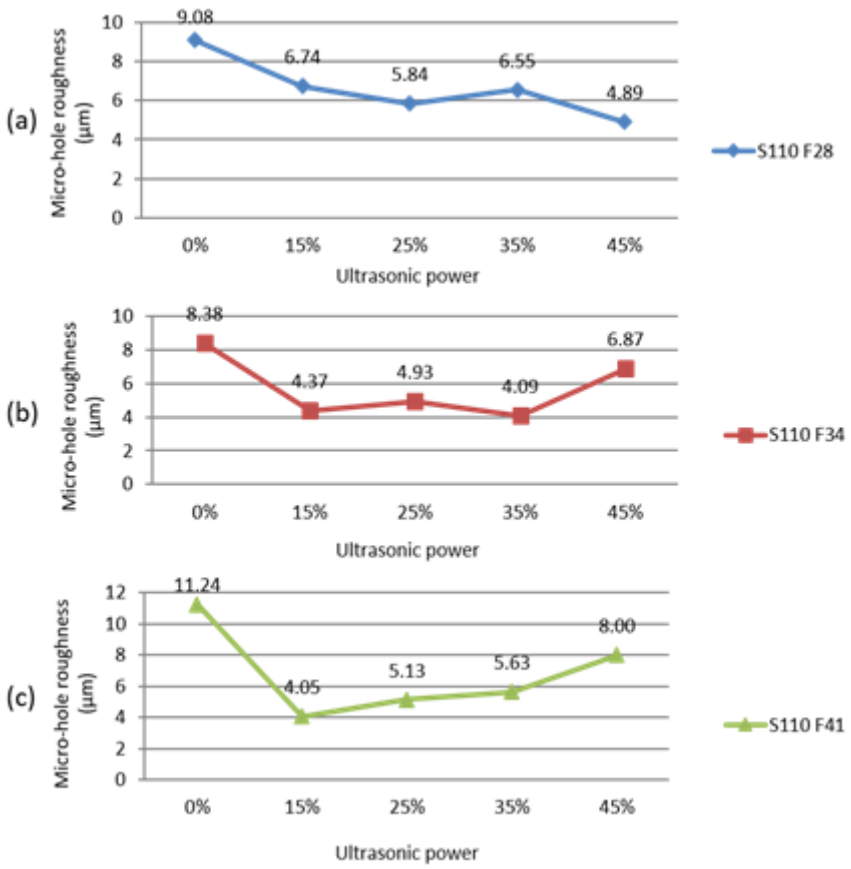

Figure 12

Micro-hole roughness of ultrasonic-assisted drilling in different feed rate.

Figure 13

Entrance burrs of ultrasonic-assisted drilling in different feed rate.

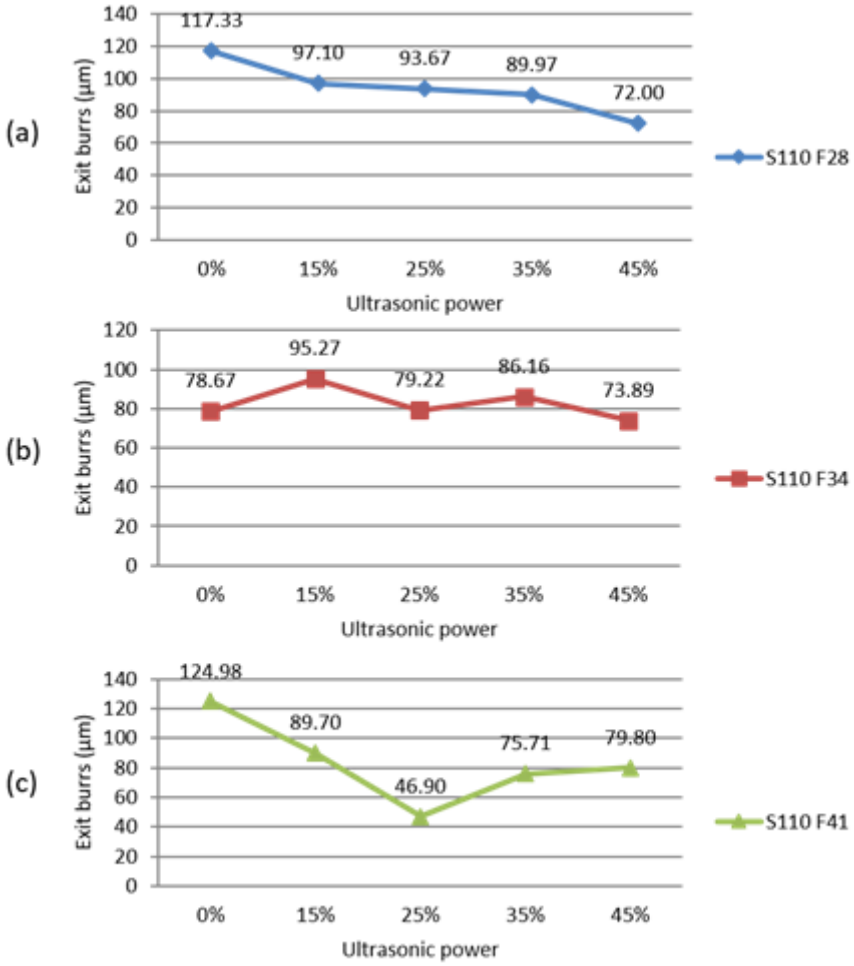

Figure 14

Exit burrs of ultrasonic-assisted drilling in different feed rate.

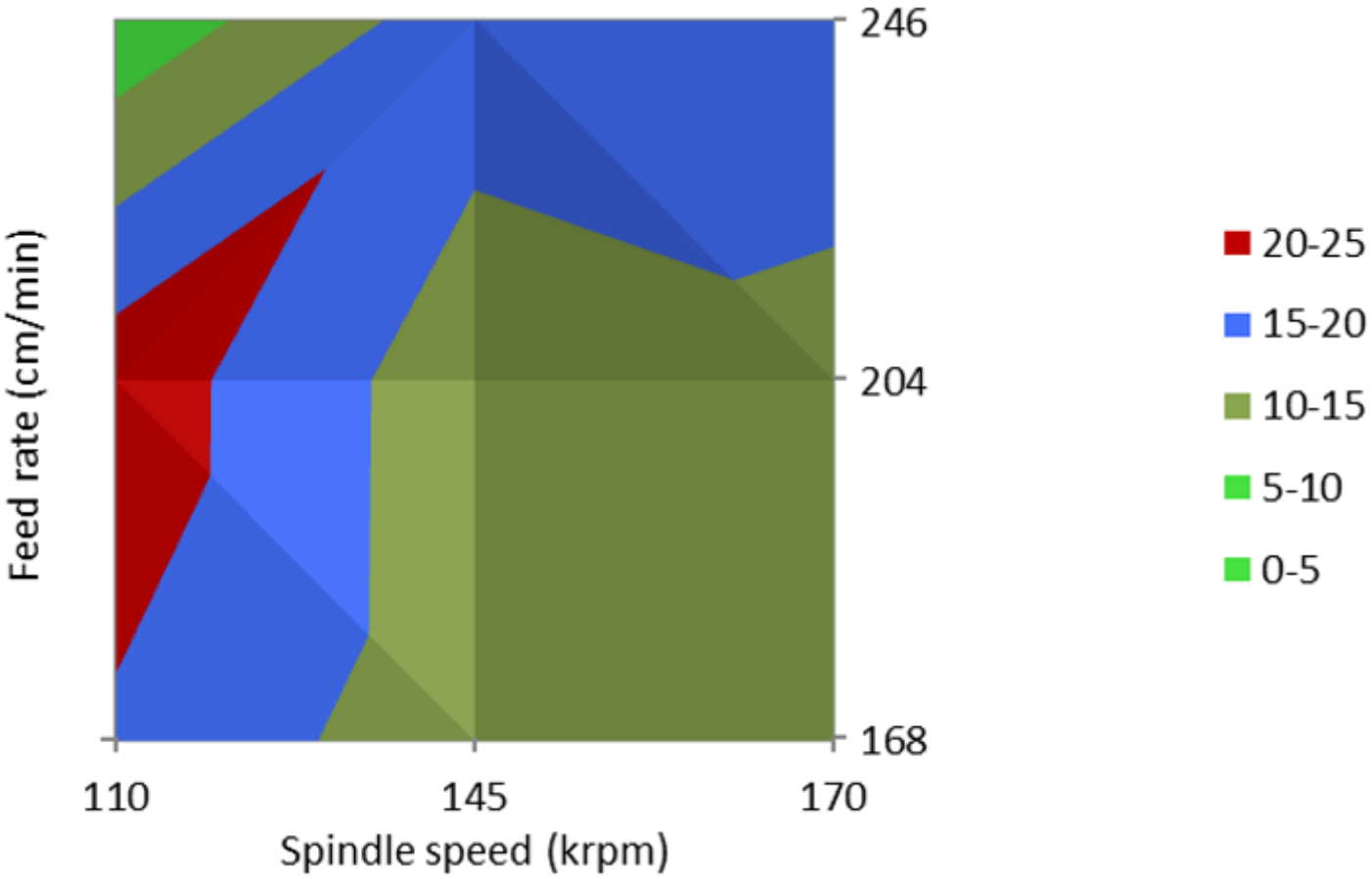

Figure 15

Comparison of entrance burrs results for ultrasonic-assisted drilling.

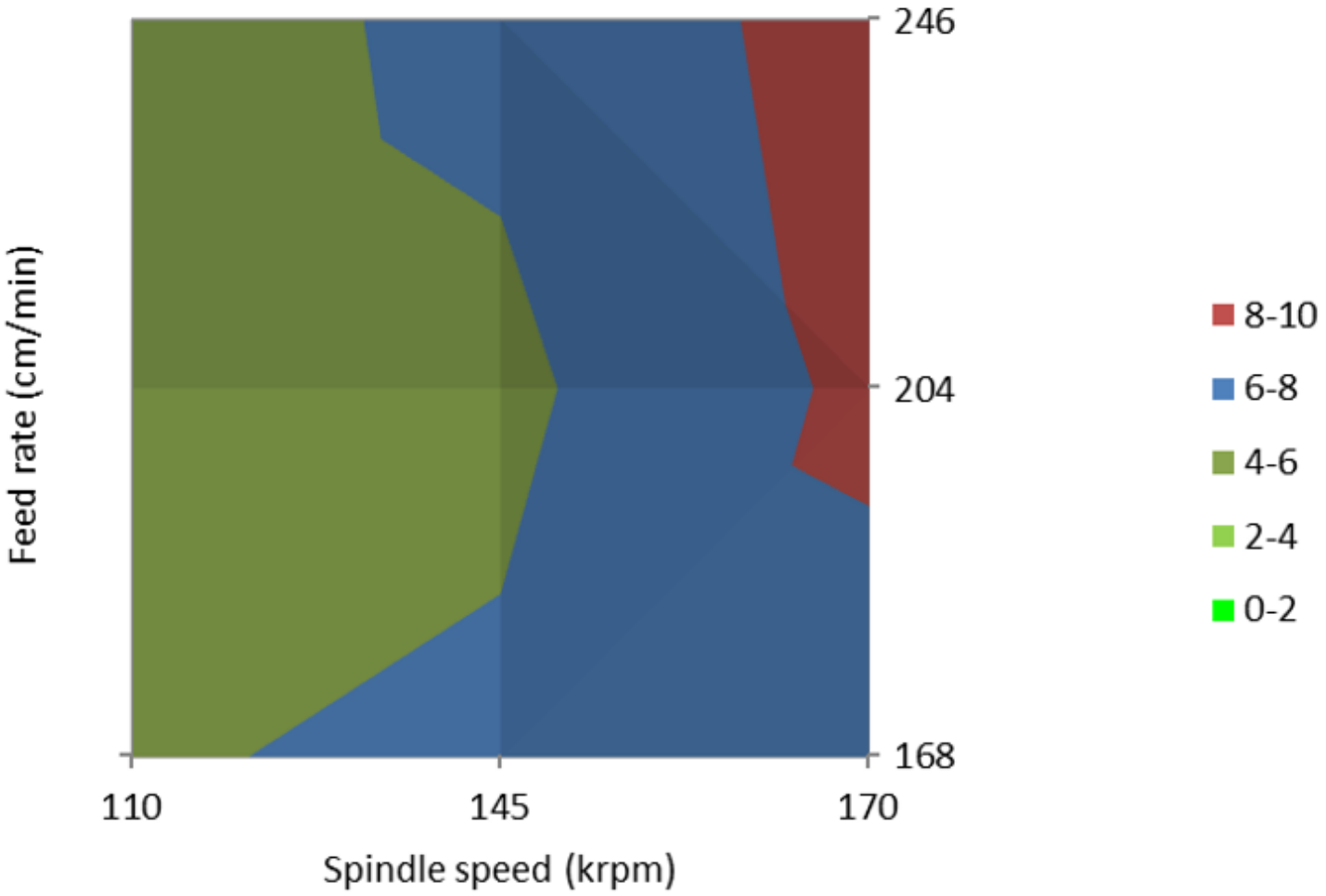

Figure 16

Comparison of Micro-hole roughness results for ultrasonic-assisted drilling.

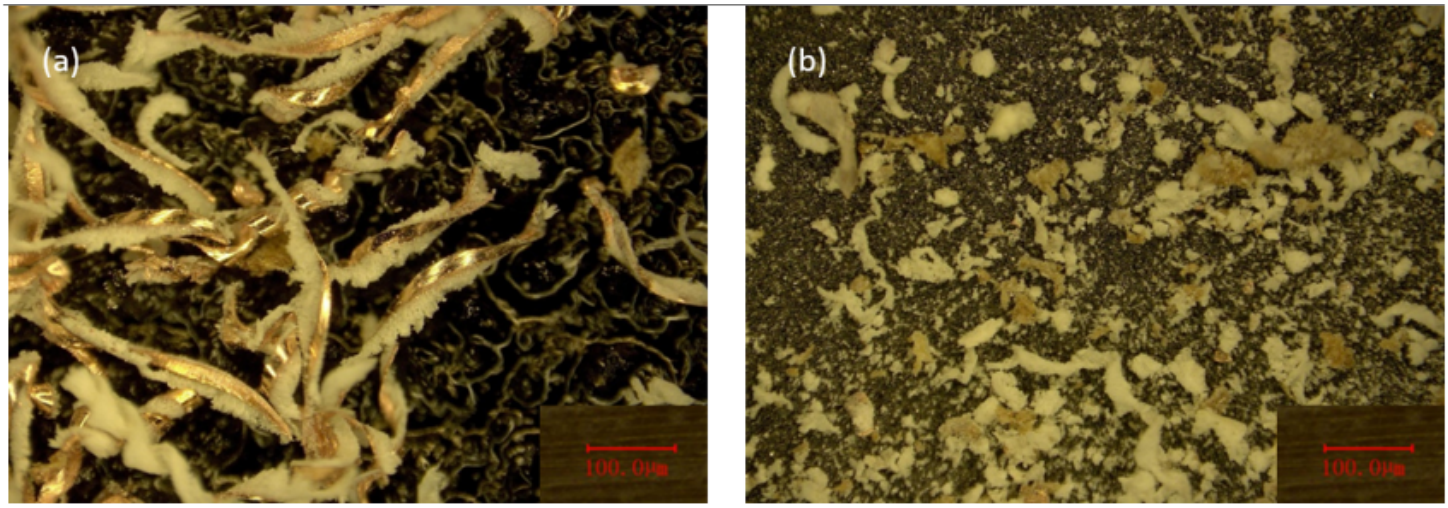

Figure 17

Comparison of drill chips between normal drilling (a) and ultrasonic-assisted drilling (b).